Coupled geomorphic and habitat response to a flood pulse revealed by remote sensing

Lee R. Harrison,[1,2] Andrew Pike,[3,1] and David A. Boughton,[1]

[1]Southwest Fisheries Science Center, National Marine Fisheries Service, National Oceanic and Atmospheric Administration, 110 Shaffer Road, Santa Cruz, CA 95060, USA

[2]Earth Research Institute, University of California, Santa Barbara, CA 93106, USA

[3]University of California, Santa Cruz, Cooperative Institute for Marine Ecosystems and Climate (CIMEC), Santa Cruz, CA 95060, USA

This is the author manuscript accepted for publication and has undergone full peer review but has not been through the copyediting, typesetting, pagination and proofreading process, which may lead to differences between this version and the Version of Record. Please cite this article as doi: 10.1002/eco.1845

Abstract. Despite a growing consensus on the importance of floods in structuring river ecosystems, predicting the geomorphic and habitat response to specific flood pulses across a range of scales remains challenging. We used a large reservoir release in a semi-arid river to characterize geomorphic and habitat responses to a flood pulse, using an integrated field, remote sensing, and modeling approach. Large-scale geomorphic changes were observed as a result of the flood, including lateral migration of the river channel, gravel bar formation and development of off-channel chutes. Spatial patterns of gravel storage varied with downstream distance from a large dam, with the upper 20 km experiencing a net sediment deficit and the lower 60 km undergoing net deposition. The longitudinal trends in gravel transport and storage reflected differences in channel gradient and predicted values of sediment mobility. The flood lowered the channel by an average of -0.5 m and roughly doubled the areal extent of pools, by incising new pools in curved reaches and in areas where the river abutted valley walls and terraces. The increased pool abundance provided greater habitat connectivity and was predicted to have positive impacts on anadromous steelhead, providing up to a 3-fold increase in the number of juvenile fish the river could support. Results from this study highlight the value of using flood pulses as opportunities to learn about river behavior, and for testing the degree to which physical processes can help restore the form and function of river ecosystems.

Keywords. connectivity, flood pulse, geomorphology, remote sensing, riverscape

1. Introduction

River ecosystems are structured by physical and biological processes that operate over a range of scales, from individual sediment grains to the entire valley floor. At the local scale, moderate flood pulses break up the river channel substrate and remove accumulated fine sediment (Wilcock *et al.*, 1996), which can be detrimental to salmon embryo survival (Sear *et al.*, 2008). The lateral migration of river channels during larger flood events scours pools and creates undercut banks (Florsheim *et al.*, 2008), which in turn provide ecologically valuable rearing habitat for salmonids (Trush *et al.*, 2000). During overbank flood events, chutes can form across gravel bars and floodplains in locations where the erosional potential of the floodwaters exceeds the resistance provided by riparian plants and floodplain topography (Constantine *et al.*, 2010). Such off-channel habitats provide important seasonally inundated floodplain habitat, which enables rapid growth in juvenile salmonids (Jeffres *et al.*, 2008). Because fish use various habitat units during daily movements and seasonal migrations, overall fish production depends not only on the availability of individual habitat patches used during a given life-stage, but also on the connectivity of habitat patches (Le Pichon *et al.*, 2009). While there has been considerable work on the role of floods in shaping river ecosystems (Yarnell *et al.*, 2015), very little is known about the effects of flood pulses on habitat patch structure and connectivity.

The physical process drivers which generate diverse, interconnected, habitat patches have been altered on a global scale by large dams (Poff *et al.*, 2010). Large dams trap the upstream

sediment supply and reduce the magnitude, frequency and duration of sediment-transporting flow events, which fundamentally alters the equilibrium between the transport capacity of the river and the sediment load (Schmidt and Wilcock, 2008). There is a large body of literature on the effects of dams on rivers, with commonly observed geomorphic effects of channel narrowing (Andrews, 1986), river bed incision (Williams and Wolman, 1984) and channel simplification (Graf, 2006). Diminished peak flows and reduced sediment supply following dam closure may also limit the development of gravel bars (Venditti *et al.*, 2012), reduce lateral channel migration (Shields *et al.*, 2000), and allow vegetation encroachment (Rood and Mahoney, 1990). The simplification of river channels below dams in turn can lead to large-scale alteration of aquatic ecosystems (Ligon *et al.*, 1995).

Controlled flow releases in regulated rivers increasingly are used by river managers in attempts to offset some of the negative effects of dams on river ecosystems, including efforts to rebuild sandbars (Grams *et al.*, 2013), enhance channel-floodplain connectivity (Opperman *et al.*, 2010), and promote native riparian plant communities (Wilcox and Shafroth, 2013). Goals of managed flow regimes initially focused on providing minimum base flows for target species, but more recently attention has shifted towards defining functional flows which link attributes of the natural flow hydrograph to specific geomorphic and ecological processes (Yarnell *et al.*, 2015). Such process-based approaches are thought to have a greater likelihood of developing self-sustaining river ecosystems (Beechie *et al.*, 2010).

Despite growing consensus for the need of process-based flow management, understanding and predicting how a river ecosystem will respond to a given flood pulse is a challenging task, requiring mechanistic linkages between streamflow, river morphology, and habitat generation. The role of flood pulses in shaping river morphology depends on a number of physical factors, including the discharge magnitude and duration, sediment supply, river gradient, valley confinement, and flow resistance provided by riparian vegetation (Hooke, 2015). Depending on the sensitivity of the river to change, river channels can experience large-scale adjustments, which reset the channel morphology (Dean and Schmidt, 2013), or relatively minor changes that maintain the existing morphology (Magilligan *et al.*, 1998). Similarly, while some studies have reported an increase in the quality and productivity of salmonid spawning habitat in response to flood events (Ortlepp and Murle, 2003), other studies have found that the overall quality and areal extent of pre- and post-flood fish habitat tends to be approximately the same (Wheaton *et al.*, 2010a; Mandlburger *et al.*, 2015). Large-scale flow experiments offer a potential framework for reducing the uncertainty in flow management by establishing process-based linkages between floods and habitat generation, and for testing and refining predictive models (Konrad *et al.*, 2011; Olden *et al.*, 2014). Yet few studies have quantified the coupled geomorphic and habitat responses to flood pulses across spatial scales.

Remotely sensed data offer the ability to characterize fluvial systems in high resolution (1 m) over large spatial scales (Carbonneau *et al.*, 2012), which is key for understanding the governing processes that structure river ecosystems (Fausch *et al.*, 2002). For example, aerial imagery has

been used to map sediment grain-size (Dugdale *et al.*, 2010), in-stream-habitats and the distribution of large wood (Marcus *et al.*, 2003), and habitat heterogeneity at the riverscape scale (Hugue *et al.*, 2016). Multispectral and hyperspectral imagery have been used to map water depths by correlating field measurements of depth with the ratio of two spectral bands (Gilvear *et al.*, 2007; Legleiter *et al.*, 2009). Airborne Light Detection and Ranging (LiDAR) data have become the standard in quantifying topography (Passalacqua *et al.*, 2015) and vegetation extent and structure (Bertoldi *et al.*, 2011), and LiDAR data has been used to evaluate the geomorphic response to flood events through the use of multitemporal remote sensing campaigns (Croke *et al.*, 2013; Perignon *et al.*, 2013). Bathymetric LiDAR sensors have also been used to support the development of two-dimensional hydrodynamic models (McKean *et al.*, 2014) and to map the spatial distribution, patch size and connectivity of aquatic habitats (Carnie *et al.*, 2015).

When combined with process-based ecological models (Railsback *et al.*, 2003), remote sensing holds the potential to examine how flood pulses re-structure fish habitats over large spatial extents with fine resolution, potentially giving insight into how physical processes relate to the development of high-quality habitat. Despite the promise of remote sensing, we are unaware of previous work that has documented how flood pulses influence the total number, capacities, and connectivity of aquatic habitats in high-resolution at the riverscape scale. Here we use an unplanned reservoir release on a semi-arid, alluvial river as a field-scale experiment, using remote sensing to gain insight into the geomorphic response to a large, infrequent flood

event, and the resulting effects on juvenile salmonid habitat patch structure and connectivity. This work was motivated by the following questions:

1. What are the primary geomorphic processes triggered by a large flood pulse?
2. How do flood-generated, geomorphic processes influence salmonid habitat quality, connectivity and production?

2. Methods

2.1 Study Area

The Santa Ynez River flows west 149 km from headwaters in the Transverse Ranges of southern California to the Pacific Ocean, draining 2,320 km^2 and alternating between confined and unconfined alluvial valley reaches. This study focused on the lower 80 km of the mainstem between Bradbury Dam and the Pacific Ocean (Figure 1). Morphology varies along the length of the lower river, having a gravel-bed with alternating pool-riffle sequences and a sparsely vegetated floodplain. The channel migrates laterally during infrequent flood events, scouring pools, building gravel bars and recruiting large wood via bank migration. Between floods, dense, shrubby vegetation colonizes the low-flow channel. Additional site characteristics are provided in Table 1.

Flow regulation following the construction of Bradbury Dam in 1953 reduced the magnitude and frequency of channel-shaping floods in the river, with the 2, 5 and 10 year floods having

decreased by 30 - 40% in the post-dam era. Bradbury Dam is a ~60 m high structure, which stores up to ~2.4 x 10^8 m^3 of water in Lake Cachuma. Water is stored during the wet winter months and released in the dry summer months to support agriculture and other municipal uses in the watershed. The sediment discharge has been reduced by approximately 50% in the post-dam era (Willis and Griggs, 2003), though several unregulated tributaries enter the Santa Ynez River below Bradbury Dam (Figure 1b), delivering a mixture of sand through cobble-sized bed material to the mainstem river. Sediment delivery from tributaries can be particularly high during El Niño Southern Oscillation (ENSO) years, when heavy rainfall can trigger numerous landslides that transfer large volumes of sediment from hillslopes to the valley floor (Gabet and Dunne, 2002).

Anadromous steelhead (*O. mykiss*) use the lower 80 km of the Santa Ynez River to complete the freshwater portion of their lifecycle. In this region the anadromous steelhead life-cycle consists of upstream migration of adults from the Pacific Ocean in January through April each year, followed by immediate spawning in gravel substrates of riffles and pool tails. Egg incubation and early juvenile development in the gravel occurs in the spring, with subsequent dispersal of juveniles in May and June from spawning areas to pool habitats for the duration of the summer low-flow season and the following rainy season (Boughton *et al.*, 2006). Juveniles typically spend one to two years in freshwater before growing to a sufficient size to trigger physiological transformation to smolts, a saltwater form that migrates back downstream to the ocean, where they spend one to two years maturing into adults (Satterthwaite *et al.*, 2009).

Although limiting factors for steelhead production in the river are only beginning to be investigated systematically (Boughton *et al.*, 2015), it seems likely that one of the most important limiting factors is the carrying capacity and connectivity of pools during the summer low-flow season. Connectivity of pool habitat is structured by the length and flow volume of riffles separating them, and allows the species to respond adaptively to deteriorating conditions in individual pools by moving to other, often deeper or cooler pools (Hwan and Carlson, 2016). Juvenile salmonids are highly territorial such that the amount of usable channel space tends to regulate abundance (Chapman, 1966), and the summer low-flow season is when the extent of wetted habitats is at a minimum (Boughton *et al.*, 2009; Hwan and Carlson, 2016). Moreover, although accessibility of habitats by migrating adults can also be a limiting factor in dry years with low spring flows, the fecundity of individual adult steelhead is sufficiently high (2,000 – 11,500 eggs per female; (Shapovalov and Taft, 1954)) that only a modest number of spawning females, and modest amount of spawning habitat are typically needed to saturate available pool habitat during summer low-flows. Young-of-the year expiring in drying stream reaches is a common summertime occurrence in southern California (Boughton *et al.*, 2009), and while unsuitable water temperature in summer can also be an important limiting factor in this region, it does not itself limit steelhead productivity in the Santa Ynez River (Boughton *et al.*, 2015). Management practices favoring introduced warm-water game fishes in the river may limit pool use by juvenile steelhead (Boughton *et al.*, 2015). However, before addressing biological

limiting factors such as predation by exotic species, there is an existing need to establish the physical habitat potential of the river system, which is the aim of the present paper.

2.2 2011 flood

During the winter of 2011 a series of intense storms required sustained high flow releases to maintain capacity for water storage in Lake Cachuma. A peak flow of 762 m^3 s^{-1} was recorded at the USGS gage at the Narrows, near Lompoc (#11133000) on March 21, 2011, with mean daily discharge values remaining above baseflow conditions for over two months. The instantaneous peak flow had a recurrence interval of slightly above 10 years as determined from a log Pearson type III analysis calculated from the post-dam annual peak flow data (1953 - 2015). The flood caused extensive erosion and deposition, lateral migration, and channel reworking in the lower mainstem river and floodplain.

2.3 Remote sensing data

On July 30, 2010, airborne near-infrared (NIR) LiDAR data and multispectral imagery were collected from Bradbury Dam to the Pacific Ocean, providing full coverage of the lower 80 km of the river and valley floor. A second, post-flood data set was obtained on August 1st, 2011, over the same extent. The LIDAR data consisted of bare-earth, digital elevation models (DEMs) with 1 m grid cells and the imagery consisted of true color images with 0.5 m pixels. LiDAR and image data were collected when much of the river corridor was dry (<5% of the valley floor

was inundated during both flights) and turbidity and water depths were low, providing ideal conditions for acquiring remotely sensed data.

2.4 Ground survey data

We conducted pre- and post-flood ground surveys within one month after the 2010 and 2011 remote sensing flights using real-time kinematic (RTK) global positioning systems (GPS) to survey topography in areas of the river that were submerged during the flights and to obtain a census of pool habitats. We focused the ground surveys on the Refugio-Alisal reach (orange line Figure 1c), which is thought to provide the highest quality steelhead habitat in the project area (Robinson *et al.*, 2009), with topographic data collected at transects spaced every 15 m over a 6.8 km sub-reach. The survey points were converted from Cartesian coordinates to a flow-oriented, curvilinear coordinate system, which was referenced to the channel centerline, then a triangular irregular network (TIN) was generated using Delaunay Triangulation. The resulting TIN was converted to a raster DEM with 1 m spatial resolution. These DEMs were used to map pools and assist in geomorphic process and habitat change interpretations.

2.5 Water depth estimation

In order to fully analyze the geomorphic and ecologic responses to the flood, beyond the limited extent of our field data, we needed to characterize water depth in areas submerged during the flights. Water depth was estimated using a spectrally-based remote sensing technique that

relates measured water depths (d) to an image-derived quantity (Winterbottom and Gilvear, 1997; Legleiter *et al.*, 2009):

$$X = \ln\left[\frac{R(\lambda_1)}{R(\lambda_2)}\right] \quad (1)$$

where $R(\lambda_1)$ and $R(\lambda_2)$ are the reflectance values of spectral bands within an image. Values of X were calculated using the green band as the numerator [$R(\lambda_1)$] and the red band as the denominator [$R(\lambda_2)$] in equation (1). Field measurements were used to develop calibration relationships between d and X, using depths measured along the Refugio-Alisal reach using RTK GPS, collected within one week of the 2010 flight (n = 165) and on the day of the 2011 flight (n = 142). Regression analysis was used to determine the best fit line between measured values of d and X, selecting half of the water depths at random from each data set to perform the calibration, with the remainder used to assess the depth retrieval accuracy (Legleiter, 2012). We found good agreement between calibrated values of X and d for both the 2010 and 2011 data sets using quadratic functions, with R^2 values of 0.74 and 0.75, and regression standard error (σ_r) values of 0.14 m and 0.15 m. Comparison between measured and predicted depths also showed close agreement, with R^2 values of 0.73 and 0.7 and root mean square errors (RMSE) of 0.15 and 0.16 m for the 2010 and 2011 validation data sets. The measured versus predicted regression slope and intercept values were close to 1 and 0, respectively, indicating that the depth retrieval was unbiased (see summary provided in Table 2). The calibrated relationships between d and X were applied to all of the wetted pixels in the 2010 and 2011 images to obtain continuous maps of the

water depth. These depth maps were then subtracted from the NIR LiDAR water surface elevations, which resulted in continuous maps of the river bathymetry along the wetted channel.

2.6 Quantifying geomorphic change

Spatial patterns of erosion and deposition were calculated for the 80 km mainstem channel and floodplain, using LiDAR data for the dry portions of the project area and the spectrally-derived bathymetry in the wetted portions of the channel. A DEM of difference (DoD) was generated by subtracting the post- from the pre-flood DEM, using the approach of *Wheaton et al*., (2010b). We assigned a spatially uniform error of 0.15 m to both pre and post-flood DEMs, then used the error-propagation approach of *Brasington et al*., (2003) to estimate the minimum level of change detectable above the noise of the data. The uncertainty in the DoD was approximated using a probabilistic thresholding approach (after *Lane et al*., (2003)), set at the 95% confidence interval. The probabilistic thresholding resulted in discarding any elevation differences having a greater than 5% probability of occurring by chance alone, which in our case resulted in omitting elevation change observations between -0.42 m to 0.42 m in the DoD. Volumetric changes in erosion and deposition were calculated for each cell by multiplying the change in bed elevation times the area of each cell (1 m^2), using only those cells where the elevation change exceeded the critical level of detection.

2.7 Sediment mobility predictions

To aid interpretation of the measured morphologic changes we performed a suite of steady-flow simulations with varying recurrence intervals (Q_2 - Q_{10}), spanning the range of potential sediment-transporting discharges in the 2011 flow event. We constructed a one-dimensional (1D), HEC-RAS (http://www.hec.usace.army.mil/software/hec-ras/documentation.aspx) model using the 2011 bathymetry, with cross-sections extracted every 30 m. The flow model was calibrated by adjusting the flow resistance (specified as Manning's *n* values for the channel and floodplain) to minimize the error between measured stage data collected at the USGS gage near Solvang (#11128500), with a RMSE of 0.15 m.

We used the flow model to calculate the likelihood of sediment mobility using the Shields stress (τ^*):

$$\tau^* \equiv \frac{\tau_b}{(\rho_s - \rho)gD} \quad (2)$$

where τ_b = the bed shear stress (N m^{-2}), ρ_s is the density of sediment (kg m^{-3}), ρ is the density of water (kg m^{-3}), g is acceleration due to gravity (m s^{-2}), and D (m) is the sediment grain size. Grain-size distributions were obtained from 6 standard Wolman pebble counts and 27 photos collected on exposed gravel bars and riffles, which were processed using the digital grain-size algorithm of Graham *et al*., (2005). Field data indicated that the particle diameter decreased with distance from Bradbury Dam, and a simple exponential function, developed by Sternberg in 1875, was employed to estimate the pattern of longitudinal, downstream fining (Hoey and Bluck, 1999; Constantine *et al.*, 2003):

$$D = D_0 e^{-al} \quad (3)$$

where D is a characteristic sediment diameter (m), l is distance downstream (km), D_0 is the grain-size (m) at the upstream end of the reach (l = 0), and a is a diminution coefficient (km^{-1}) that represents the effects of sediment sorting and abrasion. The exponential trend was fitted to the grain-size data by least squares linear regression (R^2 = 0.79). Values of D were then estimated at each HEC-RAS cross-section using equation (3), and these spatially explicit values of D were used in estimates of the Shields stress (τ^*) via equation (2). Sediment was assumed to be mobile when τ^* values equaled or exceeded a critical Shields stress (τ^*_c), of 0.03 after *Buffington and Montgomery* (1997).

2.8 Changes in pool habitat and connectivity

Individual pools were identified from the ground survey data by digitizing the pool area based on contour maps derived from the pre- and post-flood RTK GPS data described in section 2.4. Pools also were identified using the LiDAR and imagery datasets for the mainstem between Bradbury Dam and the Ocean. For this portion of the analysis, we developed a pool identification algorithm based on measured water surface elevation (WSE) values from the aerial LiDAR, and estimates of the water depth described in Section 2.5. The predicted depth was subtracted from the WSE values to obtain an estimate of the river bed height in 1 m increments along the thalweg. The raw river bed height values were smoothed over 50 m intervals. We then used the smoothed bed height values to calculate the streamwise curvature of the river bed elevation values (change in slope with respect to streamwise distance) over 1 m intervals. Pools

were identified as river segments with positive curvature (i.e. concave bed profile) that also met the criterion that the depth > 0.3 m. The pool identification algorithm was used to first identify pools along the channel thalweg, based on the curvature and depth criteria. Once pools were identified along the thalweg, we extracted all of the water depth values over the entire wetted extent of each pool to determine the area and volume of each individual pool. In order to test the predictive capability of this technique, measured values of pool abundance and length obtained via the ground survey data were compared to the predictions made for the 2010 and 2011 data sets. The pool mapping approach used here is similar to that of McKean *et al*., (2009) who used river bed concavities, derived from a bathymetric LiDAR DEM, to identify pools along Bear Valley Creek in Idaho, USA.

In order to further explore how the flood pulse influenced the spatial distribution of habitats, we quantified the connectivity between pool habitats before and after the flood. Connectivity describes the spatial relationships of habitat patches, in our case pools, based on the size and distances between habitat patches. A dimensionless proximity index (P_x) was calculated for each pool as (Le Pichon *et al.*, 2009):

$$P_x = \sum_{i=1}^{n} \frac{A_i}{D_{ix}^2} \quad (4)$$

where n is the number of pools, x is the subject pool, A_i is the total pool area (m^2) of the ith pool, D_{ix} (m) is the distance between the nearest pool and the subject pool. Values of P_x were calculated for each pool identified in the 2010 and 2011 channel.

2.9 Steelhead smolt-production capacity

We determined how the flood affected the river's capacity to produce steelhead smolts, the life-history stage that migrates to the ocean prior to maturing. Capacity was based on the space-limited concept of population regulation in salmonids, in which territorial juveniles each require a minimum area of habitat that is a function of body size (Chapman, 1966; Dunham and Vinyard, 1997; Steingrimsson and Grant, 1999; Smith *et al.*, 2013; Rosenfeld, 2014; Lindeman *et al.*, 2015). Since it is generally found that territory size scales as a power function of body size, the smolt-production capacity k of a pool was estimated using the log-linear regression equation:

$$\ln(k) = \ln(T) - \alpha - \beta \ln(L), \quad (5)$$

where α and β are fitted parameters, T is the total usable area in the pool and L is the threshold body length at which juvenile steelhead physiologically transform into smolts (Satterthwaite *et al.*, 2009; Kendall *et al.*, 2015). We assumed L = 150 mm (Fork Length) (Boughton *et al.*, 2015). Usable area is typically assessed via suitable water depths and velocities, but Spina (2000, 2003) found that in the slow water velocities typical of summer and fall in southern California, juvenile steelhead were indifferent to variation in water velocity but did show strong age-specific associations with water depth. We therefore estimated usable area as solely a logistic function of water depth, using data from Spina (2000, 2003). The parameters α and β were estimated from 19 years of juvenile densities at 10 sites in the Carmel River, California USA, a coastal alluvial river that is ecologically comparable to the mainstem Santa Ynez. All computations followed Bayesian methods (Gelman *et al.*, 2004), using open-source software (R Development Core

Team, 2011; Stan Development Team, 2015b, a). The key assumption is that capacity for smolt production is set by usable space and characteristic territory sizes, rather than the supply of juvenile fish or constraints on pool use imposed by other fish species.

3. Results

3.1 Geomorphic changes

The DEM of Difference recorded a net volume change for the study area of 840,500 m^3 $\pm$ 546,100 m^3, with a mean increase in elevation of 0.24 m $\pm$ 0.16 m. The erosion and deposition patterns varied spatially and the longitudinal patterns in net sediment storage for the entire study area are shown in Figure 2a. There was little net sediment storage change in the upper 5 km where the channel is confined to a narrow valley and no sediment is supplied by tributaries, while there was a net sediment deficit between roughly 5 and 15 km downstream from the dam. A transition from net erosion to deposition occurred at roughly 15 km downstream from the dam and generally continued until the river outlet at the Pacific Ocean (Figure 2a).

Most of the sediment accumulation occurred on the floodplain, which experienced deposition over roughly 72% of the floodplain area, with a mean elevation change of 0.38 m $\pm$ 0.16 m (Figure 2b). Despite the overall pattern of net sediment accumulation, the river channel was consistently eroded, with erosion occurring over 81% of the low-flow channel area, and with a mean elevation change of -0.53 m $\pm$ 0.17 m (Figure 2b). At locations downstream of tributary junctions (vertical dotted lines in figures 2a and 2b) the river channel bed level changes tended to

increase, as pulses of sediment were delivered to the channel (Figure 2b). These patterns of erosion and deposition were the result of focused erosion along the channel thalweg and deposition on gravel bars and overbank floodplain topography. The longitudinal patterns of erosion and deposition were also influenced by two abrupt changes in the bed gradient, with the first occurring roughly 20 km from the dam near the town of Solvang, and the second occurring approximately 48.5 km from the dam, just upstream from the Narrows (Figure 2c).

Figure 3 shows examples of reach-scale geomorphic changes that resulted from the 2011 flood. The flood caused erosion and deposition of $\pm$ 2.5 m and extensive lateral migration of the active channel, particularly in areas where the valley width decreased over short distances (Figure 3a). Several off-channel chutes formed through erosion of gravel bars, as the river followed a shorter path across unvegetated bar surfaces, effectively reducing the sinuosity of the low-flow channel. Pool scour (>2 m) was observed in areas of high planform curvature on the outside of meander bends and where the river abutted the valley walls. Bar development tended to occur on the inside of the same tightly curved bends, with deposition generally ranging from 0.5 – 1 m, but reaching max deposition values > 2 m (Figure 3b). The combination of hydraulic scour in pools and sediment accretion on gravel bars increased the cross-stream relief of the bar-pool topography, defined here as the elevation difference between the pool thalweg and bar top. Values of the cross-stream-relief through bar-pool sections typically increased by ~0.5 m, with maximum increases in the cross-stream relief exceeding 2 m.

3.2 Predicted sediment mobility

The predicted sediment mobility of the active river channel is shown in Figure 4 for three different discharges with return intervals of 2, 5 and 10-years. The portion of the river channel predicted to be mobile ($\tau^*/\ \tau^*_c > 1$) increased with discharge, with 23%, 97% and 99% of the channel above the threshold of sediment motion for the 2, 5 and 10-year discharges, respectively. Mean values of the normalized Shields stress ($\tau^*/\ \tau^*_c$) were 0.8, 1.8 and 2.7 for the 2, 5 and 10-year flows. The spatial patterns of simulated sediment mobility were generally consistent with the observed bed elevation changes (Figure 2b), which indicated that the channel was consistently lowered along the majority of the river. Fluctuations in the sediment mobility of the river channel were largely due to local changes in the gradient, channel geometry and valley width.

3.3 Changes in pool habitat and connectivity

Pre and post-flood ground survey data indicated that the flood resulted in a 2.5-fold increase in the areal extent of pools within the 6.8 km Refugio-Alisal reach. Several long (>125 m) pools formed following the flood, with a maximum pool length of 174 m. In general, the pool identification algorithm was able to correctly predict the number of pools, with 82% and 100% of the number of pools in the Refugio-Alisal test reach identified from the 2010 and 2011 data sets. There was also good agreement between the measured and predicted pool lengths, with

median measured pool lengths of 21 m (2010) and 48 m (2011), compared to predicted median pool lengths of 30 m (2010) and 43 m (2011).

Figure 5 shows the spatial distribution of predicted pools per river km for both 2010 and 2011. The extent of pool habitat increased from 14% of the wetted channel in 2010 to 25% in 2011, with median pool volumes increasing from 150 m^3 $\pm$ 32 m^3 in 2010 to 230 $\pm$74 m^3 in 2011. The increased pool habitat occurred for almost the entire length of the river, though sediment deposition near river km 63 appears to have caused local pool infilling (Figure 5b). The volume and abundance of pools gradually decreased with distance from the dam, coincident with a reduction in sediment transport capacity.

The spatial distribution in pool habitat connectivity is also shown in Figure 5 for the pre and post-flood channel. The pre-flood channel contained isolated clusters of pools, separated by long distances (Figure 5a). The connectivity between pools, defined by the proximity index (P_x), was generally low in the first 10 km below Bradbury Dam, then gradually increased between ~10 – 35 km downstream from the dam, reaching a maximum value of P_x = 9.1 in the pre-flood channel (Figure 5a). The post-flood channel had greater connectivity throughout the length of the river, with connectivity values consistently increasing downstream from the dam until about 45 km before reaching a maximum P_x value = 23.2 (Figure 5b). The increased post-flood connectivity was due in large part to the shorter distance between pools (D_{ix}^2 in equation 4), which decreased by approximately 90%, while the ~50% increase in post-flood, median pool volumes appeared to play a secondary role.

3.4 Changes in steelhead habitat capacity

The estimated smolt-producing capacity for steelhead indicated that the flood increased the potential number of fish that could be supported within the river channel. Figure 6 shows the estimated smolt capacity for the pre and post-flood channel, where each data point represents an individual pool, and the data points have been sorted by order of increasing capacity and colored by the pool volume. The mean fish capacity per pool increased from 35 in 2010 to 48 in 2011, and the total modeled capacity for the river increased from ~5,000 to ~16,000 fish for the post-flood channel. These predicted changes were largely a result of the increased number of pools, which had a greater overall effect on the estimated fish capacity than the increased volume per pool.

4. Discussion

Understanding the effects of flood pulses on river ecosystems is difficult due to the challenges involved in developing process-based linkages between flow, geomorphic change, and habitat development. This study attempted to overcome these challenges by quantifying how a discrete flood pulse re-structured the morphology and steelhead habitat in a regulated, alluvial river. By integrating field and remote sensing data with hydraulic and ecological models, we showed how changes in river morphology influenced both the spatial distribution and

connectivity of pool habitats, and the ability of the river channel to support juvenile steelhead, which has not been previously accomplished in such high-resolution at the riverscape scale.

The observed flood pulse influenced the river morphology and steelhead habitat at multiple scales. At the scale of an individual habitat unit, the flood altered the shape of the existing bar-pool morphology, deepening pools and increasing the cross-stream relief. This is consistent with previous field studies which have documented the development of greater bar-pool relief in response to increased sediment supply from gravel augmentation (Gaeuman, 2013) and following dam removals (Zunka *et al.*, 2015). The geomorphic changes created a broader range of water depths, which in turn provided more favorable habitat conditions for juvenile steelhead. At the river bend scale, lateral shifting of 10s of m enhanced existing pool habitat and generated new pools along the length of the river. The flood created several chute cutoffs, which could provide valuable floodplain habitat utilized during flood events (Jeffres *et al.*, 2008). However off-channel habitats are often seasonally disconnected or temperature limiting in Mediterranean rivers (Merz *et al.*, 2015), thus their value as potential areas for rapid steelhead growth in a semi-arid river such as the Santa Ynez remains unclear.

The flood pulse also influenced the longitudinal habitat connectivity, which should aid fish movement during various portions of their life-cycle. Steelhead require not only suitable hydraulic conditions for feeding and resting but also need connectivity between habitat units, which provides access to a range of habitat types, and offers a mechanism for responding and adapting to fluctuating habitat quality throughout the year (Hwan and Carlson, 2016). There are

several ways in which the enhanced connectivity could influence steelhead in the Santa Ynez River. Greater habitat connectivity would be important during the late spring and early summer when alevins are emerging from the gravel and dispersing throughout the river in search of rearing habitat. This time of year also coincides with outmigrating smolts who require habitat connectivity as they emigrate to the Ocean. Connectivity is also important throughout the summer and fall for juveniles to use the estuary for rearing and retreat to pool habitats if conditions deteriorate. Increased connectivity should also aid returning adults during their upstream migration, as the increased number of pools and shorter distance between pools should provide more resting sites during migration. Adult steelhead often rest in large pools during spawning activities, thus the increased pool volumes and shorter distance between pools provides another ecological function of connected habitat units.

Our results found a high potential for geomorphic and habitat changes in response to a flood event, which we attribute to the sensitivity of the river channel to change, as the channel is laterally, unconstrained along much of the river corridor. Despite having roughly half of the sediment supply trapped above Bradbury Dam, the lower Santa Ynez River still receives approximately 265,360 m^3 of sand and gravel annually, compared to 545,000 m^3 in the pre-dam era (Willis and Griggs, 2003). In the observed flood event the peak flood magnitude was capable of triggering geomorphic processes and re-setting the habitat template as water and sediment were transported downstream. However, the flood duration was insufficient to transport the sediment supplied by tributaries completely through the mainstem river channel, resulting in

sediment aggradation in the lower river which exceeded the mean annual pre-dam sediment supply. Similar patterns of sediment aggradation in rivers below dams have been observed when the mainstem flow regime is out of phase with adjacent tributaries (Schmidt and Wilcock, 2008).

Given the sediment-rich environment of the Santa Ynez River, dam releases aimed at improving steelhead habitat would be most effective when timed with the delivery of water and sediment from tributaries. However, potential flow releases could coincide with the timing of steelhead egg incubation in the riverbed, which occurs between January and May. Sediment scour and fill during a flood event can cause egg mortality if the scour depth exceeds the depth of egg burial in the redd (May *et al.*, 2009). In the Santa Ynez River, the predicted sediment mobility remained over 2 times the threshold for sediment motion during the observed peak flood event for almost the entire river corridor (Figure 4c), suggesting that the median particle diameter would have been fully mobile (Wilcock and Mcardell, 1993), thus posing a potential risk of steelhead redd scour.

Several uncertainties exist in our sediment mobility predictions, which are related to the estimates of the sediment grain-size and boundary shear stress. We employed a widely used exponential function to describe the downstream changes in sediment grain-size, though we were unable to resolve local patterns of sediment sorting. Sediment is sorted into patches of finer and coarser grain-sizes, with sorting patterns depending on a number of factors, including the sediment supply, spatially variable flow fields and channel morphology (Nelson *et al.*, 2010). In our sediment mobility predictions, Shields stresses were well above the threshold for motion for

the Q_5 and Q_{10} (Figure 4b,c), therefore the results are not expected to be particularly sensitive to finer-scale sediment sorting at these discharges. Sediment mobility predictions at the Q_2 have greater uncertainty, as a larger fraction of the channel is predicted to be close to the threshold for sediment motion (Figure 4a). Additional uncertainties in the sediment mobility estimates exist in the usage of a one-dimensional flow model for computing the boundary shear stress. Flow strength may vary across the width of a channel due to differences in pool-riffle topography, water depth or flow resistance provided by the bed and bank topography, and these spatial patterns are not captured by 1D flow models (Ferguson, 2003). A multi-dimensional model could be used to resolve finer-scale flow fields, though 1D models have been applied successfully to investigate gravel mobility (Scheingross *et al.*, 2013) and the geomorphic effects of large floods (Dean and Schmidt, 2013; Thompson *et al.*, 2015; Hooke, 2016) and a 1D modeling approach was deemed appropriate for our goal of understanding the large-scale patterns in sediment mobility.

In this study, we focused on water depth as the main factor in contributing to overall habitat capacity of juvenile steelhead. This simplifying assumption does not take into account other factors such as the thermal regime and predators which can both influence the growth of juvenile steelhead. In a study of the thermal potential of the Santa Ynez River, Boughton *et al*., (2015) found that the Santa Ynez was thermally suitable but stressful for juvenile steelhead during summer months. An adaptation strategy of steelhead on the California coast is to move into thermally stratified pools during the hottest time of the day, which provide cooler water

temperatures more favorable for rapid growth (Nielsen *et al.*, 1994). On the Santa Ynez, Boughton *et al*., (2015) found that ~60% of sampled pools along the mainstem were thermally stratified, based on measured water temperature data. Several large, thermally stratified pools were filled in and abandoned during the flood in locations where the river avulsed and formed a new active channel (Tim Robinson, personal communication). While the loss of these isolated pools could locally reduce important oversummering habitat, these effects are likely outweighed by the approximate doubling of pool habitat along the river. Pool usage by juvenile steelhead on the Santa Ynez River may also be limited by exotic species such as Largemouth Bass (Boughton *et al.*, 2015), therefore the capacity estimates reported here are best viewed as the potential for the river to produce smolts in the absence of exotic fish. While we did not examine how the flood influenced the presence of non-native species, previous studies have found that flood pulses can remove exotic species and increase the abundance of native fish who have adapted to the natural flow regime (Kiernan *et al.*, 2012). Flow experiments could be used to evaluate the extent to which future changes in the flow regime reestablish native fish populations and reduce exotic fish.

Due to the extensive alteration of river ecosystems throughout the world by large dams, flow (Yarnell *et al.*, 2015) and sediment (Wohl *et al.*, 2015) management have become important tools in river restoration. Yet despite the widely accepted importance of flow pulses in generating and maintaining habitat complexity, the direct results of flood pulses have been difficult to quantify. The measurements and modeling presented here provide quantitative

estimates of the geomorphic response to a flood pulse along a semi-arid, alluvial river and the associated habitat response for juvenile steelhead. The observed flood was highly effective in generating new habitat and improving habitat connectivity, a finding which highlights the tightly coupled nature of physical processes and habitat production. The degree of habitat generation varied spatially, and understanding the continuum of processes that developed along the length of the river would not have been possible using traditional reach scale studies. The results further underscore the importance of establishing the sediment mass balance in order to aid interpretation of the ecosystem response to flooding and management of water releases aimed at improving aquatic habitats. The integrated field, remote sensing, and modeling approach provides a framework for developing process-based linkages between streamflow, river morphology, and habitat development across spatial scales and could be used in large-scale flow experiments (Konrad *et al.*, 2011) and river restoration projects that prioritize enhancing habitat diversity.

5. Conclusions

Using field and remotely sensed data, we quantified the three-dimensional morphologic changes associated with a large, overbank flood along the length of a lowland, semi-arid river. The active river channel and floodplain received over 800,000 m^3 of sediment from adjacent tributaries during the flood, and this sediment was distributed down the length of the river corridor and stored mainly on gravel bars located within the active channel and as overbank

floodplain deposits. Despite the overall net sediment aggradation, the river channel eroded by an average of ~0.5 m, indicating highly focused erosion of the thalweg, combined with bar and floodplain deposition. The geomorphic response was dictated by large-scale changes in gradient, sediment transport potential and the supply of sediment from adjacent tributaries.

To test the degree to which geomorphic processes influenced habitat development for juvenile steelhead, we mapped the extent of pools that existed before and after the flood. The areal extent of pools approximately doubled as a result of the flood, resulting in greater pool volumes and increased connectivity of pool habitats. Ecological model predictions indicated that the increase in pool habitat could provide up to a 3-fold increase in juvenile steelhead habitat capacity. Results from this study illustrate the role of flood pulses in triggering geomorphic processes that generate complex, interconnected riverine habitats across spatial scales. The results also highlight the importance of establishing the sediment mass balance in order to understand the potential for biophysical changes under natural and managed flood events.

6. Acknowledgements

We thank Anthony Spina for providing resources to acquire the remote sensing data. Ali Abrishamchi, Chris Hammersmark, Poyom Riles and Sloane Seferyn helped collect field data and Chris Campbell provided assistance post-processing the remote sensing data. We also thank Thomas Dunne and Carl Legleiter for valuable feedback on an earlier draft. The manuscript

greatly benefitted from the detailed comments and suggestions of James McKean and an anonymous reviewer.

7. References

Andrews, ED 1986. Downstream Effects of Flaming Gorge Reservoir on the Green River, Colorado and Utah. *Geological Society of America Bulletin* **97**: 1012-1023. Doi 10.1130/0016-7606(1986)97<1012:Deofgr>2.0.Co;2.

Beechie, TJ, Sear, DA, Olden, JD, Pess, GR, Buffington, JM, Moir, H, Roni, P, and Pollock, MM 2010. Process-based Principles for Restoring River Ecosystems. *Bioscience* **60**: 209-222. 10.1525/bio.2010.60.3.7.

Bertoldi, W, Gurnell, AM, and Drake, NA 2011. The topographic signature of vegetation development along a braided river: Results of a combined analysis of airborne lidar, color air photographs, and ground measurements. *Water Resources Research* **47**. Doi 10.1029/2010wr010319.

Boughton, D, Adams, P, Anderson, E, Fusaro, C, Keller, E, Kelley, E, Lentsch, L, Nielsen, J, Perry, K, Regan, H, Smith, J, Swift, C, Thompson, L, and Watson, F, 2006, Steelhead of the south-central/southern California coast: Population characterization for recovery planning.

Boughton, DA, Fish, H, Pope, J, and Holt, G 2009. Spatial patterning of habitat for Oncorhynchus mykiss in a system of intermittent and perennial streams. *Ecology of Freshwater Fish* **18**: 92-105. DOI 10.1111/j.1600-0633.2008.00328.x.

Boughton, DA, Harrison, LR, Pike, AS, Arriaza, JL, and Mangel, M 2015. Thermal Potential for Steelhead Life History Expression in a Southern California Alluvial River. *Transactions of the American Fisheries Society* **144**: 258-273. 10.1080/00028487.2014.986338.

Brasington, J, Langham, J, and Rumsby, B 2003. Methodological sensitivity of morphometric estimates of coarse fluvial sediment transport. *Geomorphology* **53**: 299-316. Doi 10.1016/S0169-555x902)00320-3.

Buffington, JM, and Montgomery, DR 1997. A systematic analysis of eight decades of incipient motion studies, with special reference to gravel-bedded rivers. *Water Resources Research* **33**: 1993-2029. 10.1029/96WR03190.

Carbonneau, P, Fonstad, MA, Marcus, WA, and Dugdale, SJ 2012. Making riverscapes real. *Geomorphology* **137**: 74-86. 10.1016/j.geomorph.2010.09.030.

Carnie, R, Tonina, D, McKean, JA, and Isaak, D 2015. Habitat connectivity as a metric for aquatic microhabitat quality: application to Chinook salmon spawning habitat. *Ecohydrology*: n/a-n/a. 10.1002/eco.1696.

Chapman, DW 1966. Food and space as regulators of salmonid populations in streams. *American Naturalist* **100**: 345-357.

Constantine, CR, Mount, MF, and Florsheim, JL 2003. The effects of longitudinal differences in gravel mobility on the downstream fining pattern in the Cosumnes River, California. *Journal of Geology* **111**: 233-241. Doi 10.1086/345844.

Constantine, JA, McLean, SR, and Dunne, T 2010. A mechanism of chute cutoff along large meandering rivers with uniform floodplain topography. *Geological Society of America Bulletin* **122**: 855-869. 10.1130/b26560.1.

Croke, J, Todd, P, Thompson, C, Watson, F, Denham, R, and Khanal, G 2013. The use of multi temporal LiDAR to assess basin-scale erosion and deposition following the catastrophic January 2011 Lockyer flood, SE Queensland, Australia. *Geomorphology* **184**: 111-126. DOI 10.1016/j.geomorph.2012.11.023.

Dean, DJ, and Schmidt, JC 2013. The geomorphic effectiveness of a large flood on the Rio Grande in the Big Bend region: Insights on geomorphic controls and post-flood geomorphic response. *Geomorphology* **201**: 183-198. 10.1016/j.geomorph.2013.06.020.

Dugdale, SJ, Carbonneau, PE, and Campbell, D 2010. Aerial photosieving of exposed gravel bars for the rapid calibration of airborne grain size maps. *Earth Surface Processes and Landforms* **35**: 627-639. 10.1002/esp.1936.

Dunham, JB, and Vinyard, GL 1997. Relationships between body mass, population density, and the self-thinning rule in stream-living salmonids. *Canadian Journal of Fisheries and Aquatic Sciences* **54**: 1025-1030.

Fausch, KD, Torgersen, CE, Baxter, CV, and Li, HW 2002. Landscapes to riverscapes: Bridging the gap between research and conservation of stream fishes. *Bioscience* **52**: 483-498. Doi 10.1641/0006-3568(2002)052[0483:Ltrbtg]2.0.Co;2.

Ferguson, RI 2003. The missing dimension: effects of lateral variation on 1-D calculations of fluvial bedload transport. *Geomorphology* **56**: 1-14.

Florsheim, JL, Mount, JF, and Chin, A 2008. Bank erosion as a desirable attribute of rivers. *Bioscience* **58**: 519-529. 10.1641/b580608.

Gabet, EJ, and Dunne, T 2002. Landslides on coastal sage-scrub and grassland hillslopes in a severe El Nino winter: The effects of vegetation conversion on sediment delivery. *Geological Society of America Bulletin* **114**: 983-990. Doi 10.1130/0016-7606(2002)114<0983:Locssa>2.0.Co;2.

Gaeuman, D 2013. High-flow gravel injection for constructing designed in-channel features. *River Research and Applications*: n/a-n/a. 10.1002/rra.2662.

Gelman, A, Carlin, JB, Stern, HS, and Rubin, DB, 2004, Bayesian Data Analysis, Boca Raton, Chapman & Hall/CRC.

Gilvear, D, Hunter, P, and Higgins, T 2007. An experimental approach to the measurement of the effects of water depth and substrate on optical and near infra-red reflectance: a field-based assessment of the feasibility of mapping submerged instream habitat. *International Journal of Remote Sensing* **28**: 2241-2256. 10.1080/01431160600976079.

Graf, WL 2006. Downstream hydrologic and geomorphic effects of large dams on American rivers. *Geomorphology* **79**: 336-360. 10.1016/j.geomorph.2006.06.022.
Graham, DJ, Rice, SP, and Reid, I 2005. A transferable method for the automated grain sizing of river gravels. *Water Resources Research* **41**. Doi 10.1029/2004wr003868.
Grams, PE, Topping, DJ, Schmidt, JC, Hazel, JE, and Kaplinski, M 2013. Linking morphodynamic response with sediment mass balance on the Colorado River in Marble Canyon: Issues of scale, geomorphic setting, and sampling design. *Journal of Geophysical Research-Earth Surface* **118**: 361-381. DOI 10.1002/jgrf.20050.
Hoey, TB, and Bluck, BJ 1999. Identifying the controls over downstream fining of river gravels. *Journal of Sedimentary Research* **69**: 40-50.
Hooke, JM 2015. Variations in flood magnitude–effect relations and the implications for flood risk assessment and river management. *Geomorphology* **251**: 91-107. http://dx.doi.org/10.1016/j.geomorph.2015.05.014.
Hooke, JM 2016. Geomorphological impacts of an extreme flood in SE Spain. *Geomorphology* **263**: 19-38. http://dx.doi.org/10.1016/j.geomorph.2016.03.021.
Hugue, F, Lapointe, M, Eaton, BC, and Lepoutre, A 2016. Satellite-based remote sensing of running water habitats at large riverscape scales: Tools to analyze habitat heterogeneity for river ecosystem management. *Geomorphology* **253**: 353-369. 10.1016/j.geomorph.2015.10.025.
Hwan, JL, and Carlson, SM 2016. Fragmentation of an Intermittent Stream During Seasonal Drought: Intra-annual and Interannual Patterns and Biological Consequences. *River Research and Applications* **32**: 856-870. 10.1002/rra.2907.
Jeffres, CA, Opperman, JJ, and Moyle, PB 2008. Ephemeral floodplain habitats provide best growth conditions for juvenile Chinook salmon in a California river. *Environmental Biology of Fishes* **83**: 449-458.
Kendall, NW, McMillan, JR, Sloat, MR, Buehren, TW, Quinn, TP, Pess, GR, Kuzishchin, KV, McClure, MM, and Zabel, RW 2015. Anadromy and residency in steelhead and rainbow trout (*Oncorhynchus mykiss*): a review of the processes and patterns. *Canadian Journal of Fisheries and Aquatic Sciences* **72**: 319-342.
Kiernan, JD, Moyle, PB, and Crain, PK 2012. Restoring native fish assemblages to a regulated California stream using the natural flow regime concept. *Ecological Applications* **22**: 1472-1482.
Konrad, CP, Olden, JD, Lytle, DA, Melis, TS, Schmidt, JC, Bray, EN, Freeman, MC, Gido, KB, Hemphill, NP, Kennard, MJ, McMullen, LE, Mims, MC, Pyron, M, Robinson, CT, and Williams, JG 2011. Large-scale Flow Experiments for Managing River Systems. *Bioscience* **61**: 948-959. 10.1525/bio.2011.61.12.5.
Lane, SN, Westaway, RM, and Murray Hicks, D 2003. Estimation of erosion and deposition volumes in a large, gravel-bed, braided river using synoptic remote sensing. *Earth Surface Processes and Landforms* **28**: 249-271. 10.1002/esp.483.

Le Pichon, C, Gorges, G, Baudry, J, Goreaud, F, and Boet, P 2009. Spatial metrics and methods for riverscapes: quantifying variability in riverine fish habitat patterns. *Environmetrics* **20**: 512-526. 10.1002/env.948.

Legleiter, CJ 2012. Mapping River Depth from Publicly Available Aerial Images. *River Research and Applications*: n/a-n/a. 10.1002/rra.2560.

Legleiter, CJ, Roberts, DA, and Lawrence, RL 2009. Spectrally based remote sensing of river bathymetry. *Earth Surface Processes and Landforms* **34**: 1039-1059. Doi 10.1002/Esp.1787.

Ligon, FK, Dietrich, WE, and Trush, WJ 1995. Downstream Ecological Effects of Dams. *Bioscience* **45**: 183-192.

Lindeman, AA, Grant, JWA, and Desjardins, CM 2015. Density-dependent territory size and individual growth rate in juvenile Atlantic salmon (Salmo salar). *Ecology of Freshwater Fish* **24**: 15-22. 10.1111/eff.12120.

Magilligan, FJ, Phillips, JD, James, LA, and Gomez, B 1998. Geomorphic and sedimentological controls on the effectiveness of an extreme flood. *Journal of Geology* **106**: 87-95.

Mandlburger, G, Hauer, C, Wieser, M, and Pfeifer, N 2015. Topo-Bathymetric LiDAR for Monitoring River Morphodynamics and Instream Habitats-A Case Study at the Pielach River. *Remote Sensing* **7**: 6160-6195. 10.3390/rs70506160.

Marcus, WA, Legleiter, CJ, Aspinall, RJ, Boardman, JW, and Crabtree, RL 2003. High spatial resolution hyperspectral mapping of in-stream habitats, depths, and woody debris in mountain streams. *Geomorphology* **55**: 363-380. Doi 10.1016/S0169-555x(03)00150-8.

May, CL, Pryor, B, Lisle, TE, and Lang, M 2009. Coupling hydrodynamic modeling and empirical measures of bed mobility to predict the risk of scour and fill of salmon redds in a large regulated river. *Water Resources Research* **45**: W05402. 10.1029/2007wr006498.

McKean, J, Nagel, D, Tonina, D, Bailey, P, Wright, CW, Bohn, C, and Nayegandhi, A 2009. Remote Sensing of Channels and Riparian Zones with a Narrow-Beam Aquatic-Terrestrial LIDAR. *Remote Sensing* **1**: 1065-1096. Doi 10.3390/Rs1041065.

McKean, J, Tonina, D, Bohn, C, and Wright, CW 2014. Effects of bathymetric lidar errors on flow properties predicted with a multi-dimensional hydraulic model. *Journal of Geophysical Research: Earth Surface*: 2013JF002897. 10.1002/2013JF002897.

Merz, JE, Delaney, DG, Setka, JD, and Workman, ML 2015. Seasonal Rearing Habitat in a Large Mediterranean-Climate River: Management Implications at the Southern Extent of Pacific Salmon (Oncorhynchus spp.). *River Research and Applications*: n/a-n/a. 10.1002/rra.2969.

Nelson, PA, Dietrich, WE, and Venditti, JG 2010. Bed topography and the development of forced bed surface patches. *Journal of Geophysical Research-Earth Surface* **115**. Doi 10.1029/2010jf001747.

Nielsen, JL, Lisle, TE, and Ozaki, V 1994. Thermally Stratified Pools and Their Use by Steelhead in Northern California Streams. *Transactions of the American Fisheries Society* **123**: 613-626. Doi 10.1577/1548-8659(1994)123<0613:Tspatu>2.3.Co;2.

Olden, JD, Konrad, CP, Melis, TS, Kennard, MJ, Freeman, MC, Mims, MC, Bray, EN, Gido, KB, Hemphill, NP, Lytle, DA, McMullen, LE, Pyron, M, Robinson, CT, Schmidt, JC, and Williams, JG 2014. Are large-scale flow experiments informing the science and management of freshwater ecosystems? *Frontiers in Ecology and the Environment* **12**: 176-185. 10.1890/130076.

Opperman, JJ, Luster, R, McKenney, BA, Roberts, M, and Meadows, AW 2010. Ecologically Functional Floodplains: Connectivity, Flow Regime, and Scale. *Journal of the American Water Resources Association* **46**: 211-226. DOI 10.1111/j.1752-1688.2010.00426.x.

Ortlepp, J, and Murle, U 2003. Effects of experimental flooding on brown trout (Salmo trutta fario L.): The River Spol, Swiss National Park. *Aquatic Sciences* **65**: 232-238. 10.1007/s00027-003-0666-5.

Passalacqua, P, Belmont, P, Staley, DM, Simley, JD, Arrowsmith, JR, Bode, CA, Crosby, C, DeLong, SB, Glenn, NF, Kelly, SA, Lague, D, Sangireddy, H, Schaffrath, K, Tarboton, DG, Wasklewicz, T, and Wheaton, JM 2015. Analyzing high resolution topography for advancing the understanding of mass and energy transfer through landscapes: A review. *Earth-Science Reviews* **148**: 174-193. http://dx.doi.org/10.1016/j.earscirev.2015.05.012.

Perignon, MC, Tucker, GE, Griffin, ER, and Friedman, JM 2013. Effects of riparian vegetation on topographic change during a large flood event, Rio Puerco, New Mexico, USA. *Journal of Geophysical Research: Earth Surface*: n/a-n/a. 10.1002/jgrf.20073.

Poff, NL, Richter, BD, Arthington, AH, Bunn, SE, Naiman, RJ, Kendy, E, Acreman, M, Apse, C, Bledsoe, BP, Freeman, MC, Henriksen, J, Jacobson, RB, Kennen, JG, Merritt, DM, O'Keeffe, JH, Olden, JD, Rogers, K, Tharme, RE, and Warner, A 2010. The ecological limits of hydrologic alteration (ELOHA): a new framework for developing regional environmental flow standards. *Freshwater Biology* **55**: 147-170. DOI 10.1111/j.1365-2427.2009.02204.x.

R Development Core Team, 2011, R: A language and environment for statistical computing.: Vienna, Austria, R Foundation for Statistical Computing.

Railsback, SF, Stauffer, HB, and Harvey, BC 2003. What Can Habitat Preference Models Tell Us? Tests Using a Virtual Trout Population. *Ecological Applications* **13**: 1580-1594.

Robinson, T, Hanson, C, Engblom, S, Volan, S, Baldrige, J, Riege, L, Wales, B, Shahroody, A, and Lawler, C, 2009, Summary and analysis of annual fishery monitoring in the lower Santa Ynez River, 1993-2004: Cachuma Conservation Release Board, Santa Barbara, California.

Rood, SB, and Mahoney, JM 1990. Collapse of Riparian Poplar Forests Downstream from Dams in Western Prairies - Probable Causes and Prospects for Mitigation. *Environmental Management* **14**: 451-464.

Rosenfeld, JS 2014. Modelling the effects of habitat on self-thinning, energy equivalence, and optimal habitat structure for juvenile trout. *Canadian Journal of Fisheries and Aquatic Sciences* **71**: 1395-1406. 10.1139/cjfas-2013-0603.

Satterthwaite, WH, Beakes, MP, Collins, EM, Swank, DR, Merz, JE, Titus, RG, Sogard, SM, and Mangel, M 2009. Steelhead Life History on California's Central Coast: Insights from a State-Dependent Model. *Transactions of the American Fisheries Society* **138**: 532-548. Doi 10.1577/T08-164.1.

Scheingross, JS, Winchell, EW, Lamb, MP, and Dietrich, WE 2013. Influence of bed patchiness, slope, grain hiding, and form drag on gravel mobilization in very steep streams. *Journal of Geophysical Research: Earth Surface*: n/a-n/a. 10.1002/jgrf.20067.

Schmidt, JC, and Wilcock, PR 2008. Metrics for assessing the downstream effects of dams. *Water Resources Research* **44**. Doi 10.1029/2006wr005092.

Sear, DA, Frostick, LB, Rollinson, G, and Lisle, TE 2008. The Significance and Mechanics of Fine-Sediment Infiltration and Accumulation in Gravel Spawning Beds. *Salmonid Spawning Habitat in Rivers: Physical Controls, Biological Responses, and Approaches to Remediation* **65**: 149-173.

Shapovalov, L, and Taft, AC, 1954, The life histories of the steelhead rainbow trout (*Salmo gairdneri gairdneri*) and silver salmon (*Oncorhynchus kisutch*) with special reference to Waddell Creek, California, and recommendations regarding their management: State of California, Department of Fish and Game, Fish Bulletin 98.

Shields, FD, Simon, A, and Steffen, LJ 2000. Reservoir effects on downstream river channel migration. *Environmental Conservation* **27**: 54-66. Doi 10.1017/S0376892900000072.

Smith, JA, Baumgartner, LJ, Suthers, IM, Fielder, DS, and Taylor, MD 2013. Density-Dependent Energy Use Contributes to the Self-Thinning Relationship of Cohorts. *American Naturalist* **181**: 331-343. 10.1086/669146.

Spina, AP 2000. Habitat partitioning in a patchy environment: considering the role of intraspecific competition. *Environmental Biology of Fishes* **57**: 393-400.

Spina, AP 2003. Habitat associations of steelhead trout near the southern extent of their range. *California Fish and Game* **89**: 81-95.

Stan Development Team, 2015a, RStan: the R interface to Stan, Version 2.8.0.

Stan Development Team, 2015b, Stan: A C++ Library for Probability and Samping, Version 2.8.0.

Steingrimsson, SO, and Grant, JWA 1999. Allometry of territory size and metabolic rate as predictors of self-thinning in young-of-the-year Atlantic salmon. *Journal of Animal Ecology* **68**: 17-26.

Thompson, CJ, Fryirs, K, and Croke, J 2015. The Disconnected Sediment Conveyor Belt: Patterns of Longitudinal and Lateral Erosion and Deposition During a Catastrophic Flood in the Lockyer Valley, South East Queensland, Australia. *River Research and Applications*: n/a-n/a. 10.1002/rra.2897.

Trush, WJ, McBain, SM, and Leopold, LB 2000. Attributes of an alluvial river and their relation to water policy and management. *Proceedings of the National Academy of Sciences of the United States of America* **97**: 11858-11863.

Venditti, JG, Nelson, PA, Minear, JT, Wooster, J, and Dietrich, WE 2012. Alternate bar response to sediment supply termination. *Journal of Geophysical Research-Earth Surface* **117**. Doi 10.1029/2011jf002254.

Wheaton, JM, Brasington, J, Darby, SE, Merz, J, Pasternack, GB, Sear, D, and Vericat, D 2010a. Linking Geomorphic Changes to Salmonid Habitat at a Scale Relevant to Fish. *River Research and Applications* **26**: 469-486. 10.1002/rra.1305.

Wheaton, JM, Brasington, J, Darby, SE, and Sear, DA 2010b. Accounting for uncertainty in DEMs from repeat topographic surveys: improved sediment budgets. *Earth Surface Processes and Landforms* **35**: 136-156. 10.1002/esp.1886.

Wilcock, PR, Kondolf, GM, Matthews, WVG, and Barta, AF 1996. Specification of sediment maintenance flows for a large gravel-bed river. *Water Resources Research* **32**: 2911-2921.

Wilcock, PR, and Mcardell, BW 1993. Surface-Based Fractional Transport Rates - Mobilization Thresholds and Partial Transport of a Sand-Gravel Sediment. *Water Resources Research* **29**: 1297-1312. Doi 10.1029/92wr02748.

Wilcox, AC, and Shafroth, PB 2013. Coupled hydrogeomorphic and woody-seedling responses to controlled flood releases in a dryland river. *Water Resources Research*: n/a-n/a. 10.1002/wrcr.20256.

Williams, GP, and Wolman, MG, 1984, Downstream effects of dams on alluvial rivers.

Willis, CM, and Griggs, GB 2003. Reductions in fluvial sediment discharge by coastal dams in California and implications for beach sustainability. *Journal of Geology* **111**: 167-182. Doi 10.1086/345922.

Winterbottom, SJ, and Gilvear, DJ 1997. Quantification of channel bed morphology in gravel-bed rivers using airborne multispectral imagery and aerial photography. *Regulated Rivers-Research & Management* **13**: 489-499. Doi 10.1002/(Sici)1099-1646(199711/12)13:6<489::Aid-Rrr471>3.0.Co;2-X.

Wohl, E, Bledsoe, BP, Jacobson, RB, Poff, NL, Rathburn, SL, Walters, DM, and Wilcox, AC 2015. The Natural Sediment Regime in Rivers: Broadening the Foundation for Ecosystem Management. *Bioscience* **65**: 358-371. 10.1093/biosci/biv002.

Yarnell, SM, Petts, GE, Schmidt, JC, Whipple, AA, Beller, EE, Dahm, CN, Goodwin, P, and Viers, JH 2015. Functional Flows in Modified Riverscapes: Hydrographs, Habitats and Opportunities. *Bioscience* **65**: 963-972. 10.1093/biosci/biv102.

Zunka, JPP, Tullos, DD, and Lancaster, ST 2015. Effects of sediment pulses on bed relief in bar-pool channels. *Earth Surface Processes and Landforms* **40**: 1017-1028. 10.1002/esp.3697.

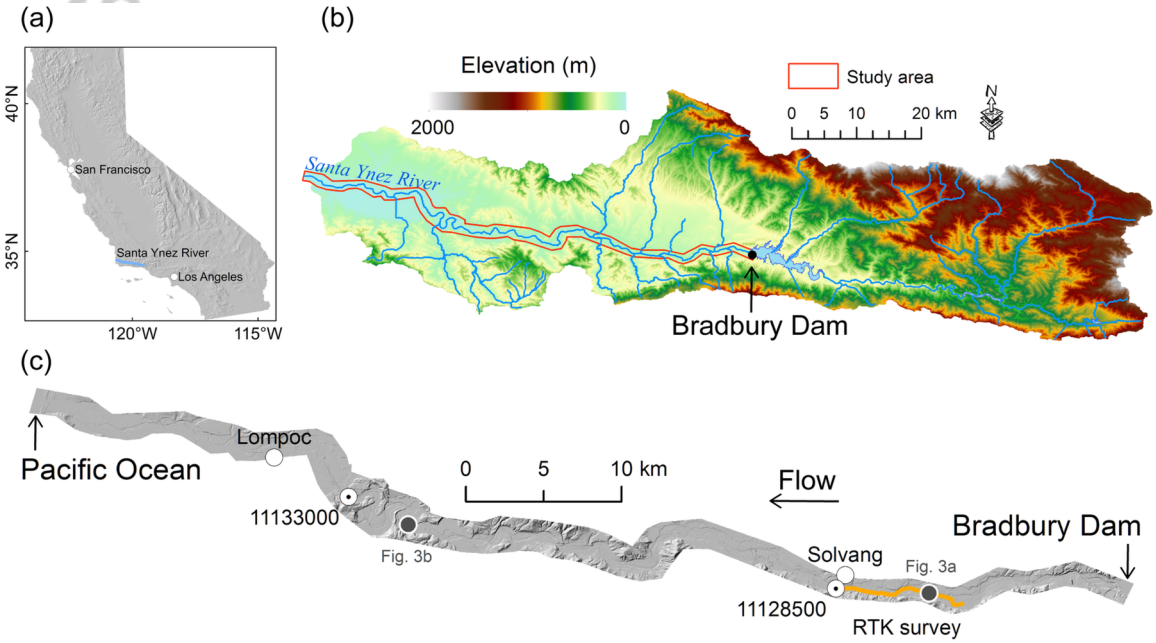

ECO_1845_F1.tif

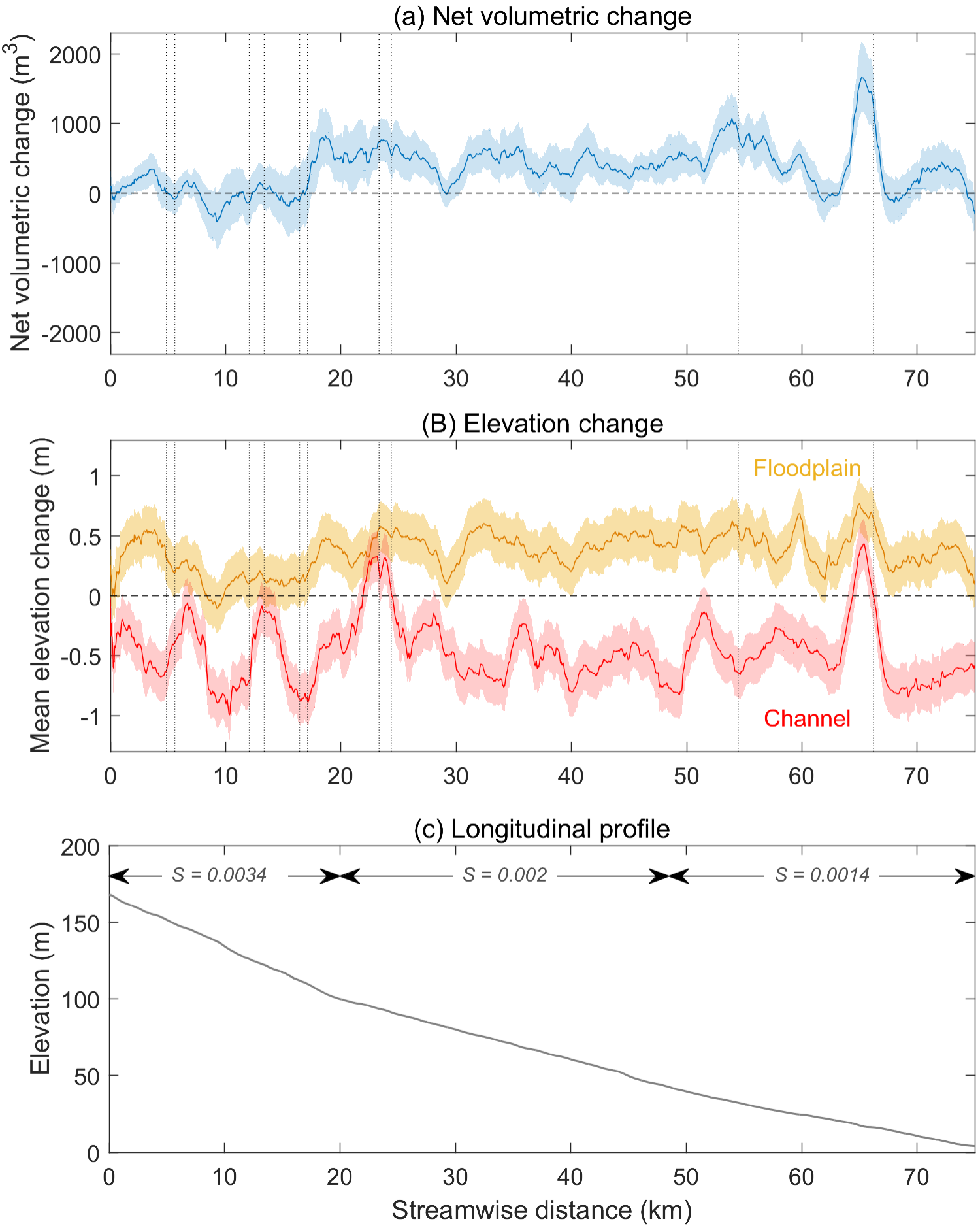

ECO_1845_F2.tif

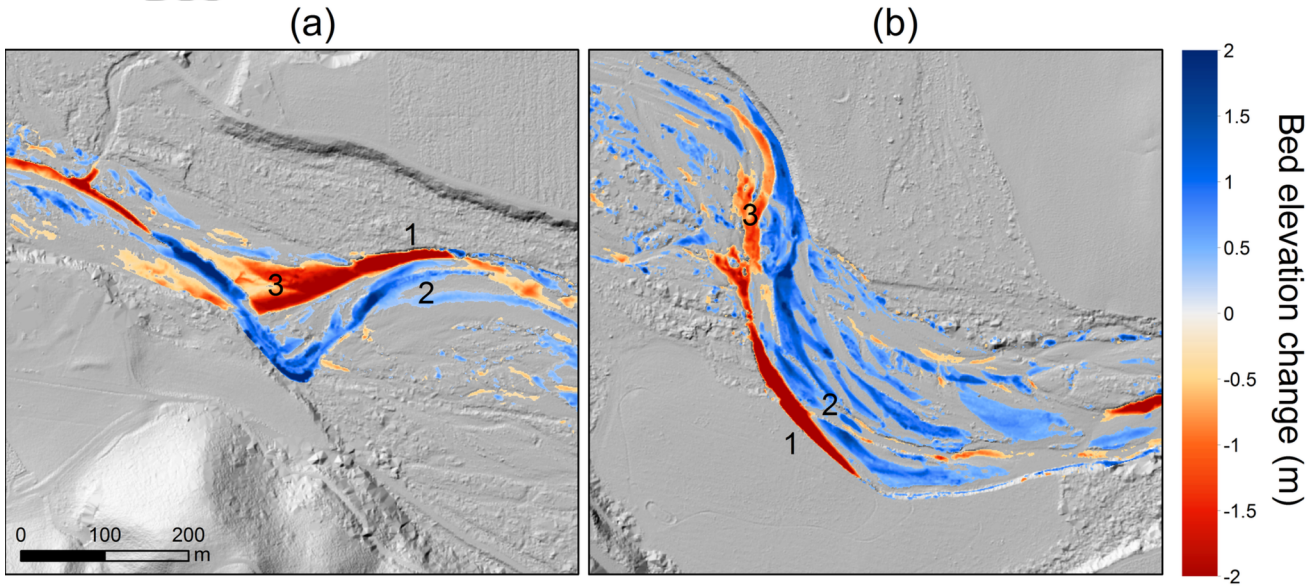

ECO_1845_F3.tif

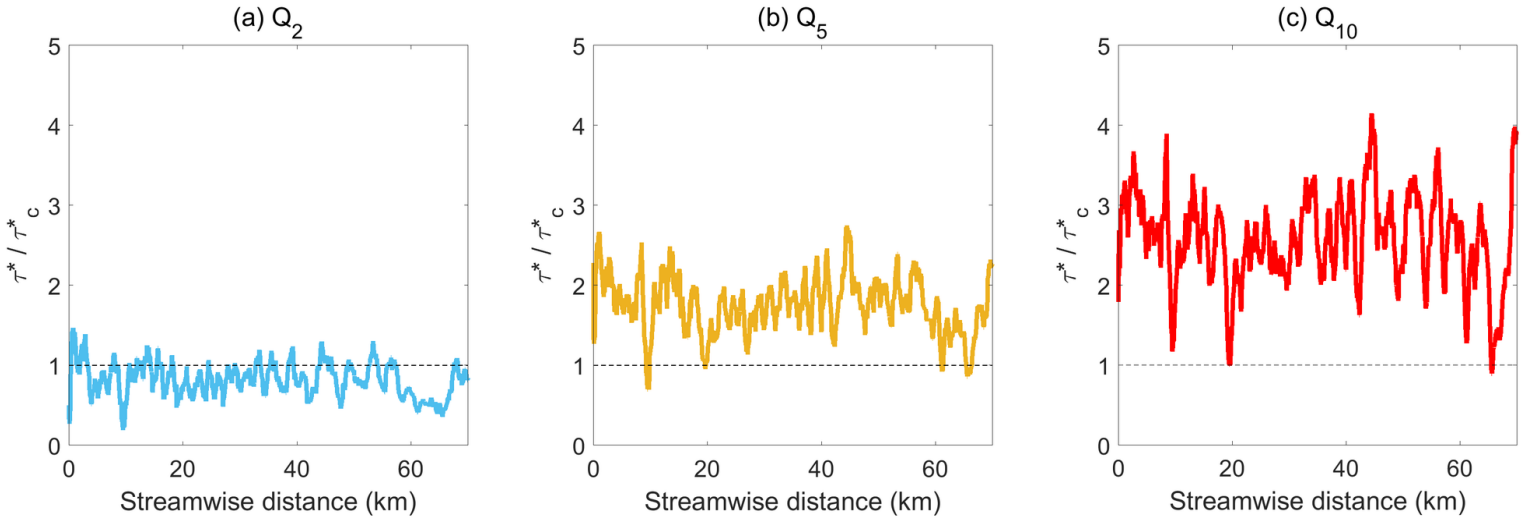

ECO_1845_F4.tif

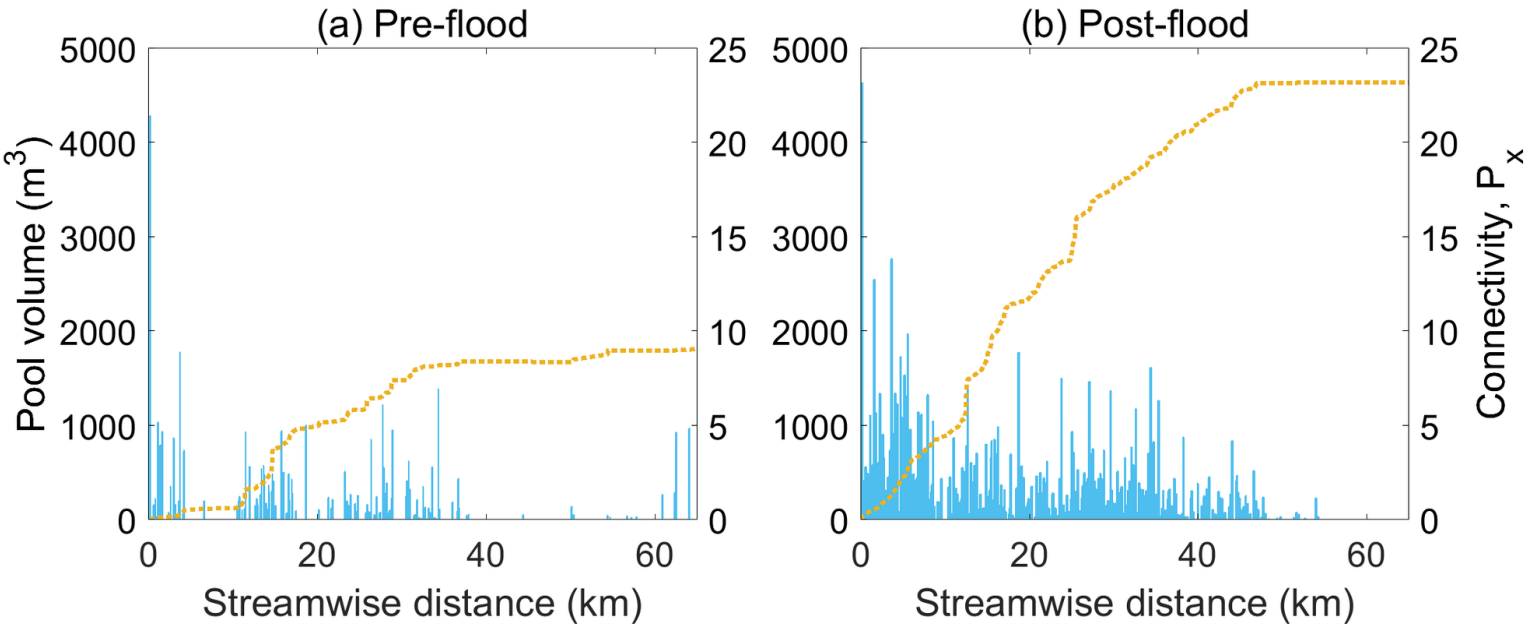

ECO_1845_F5.tif

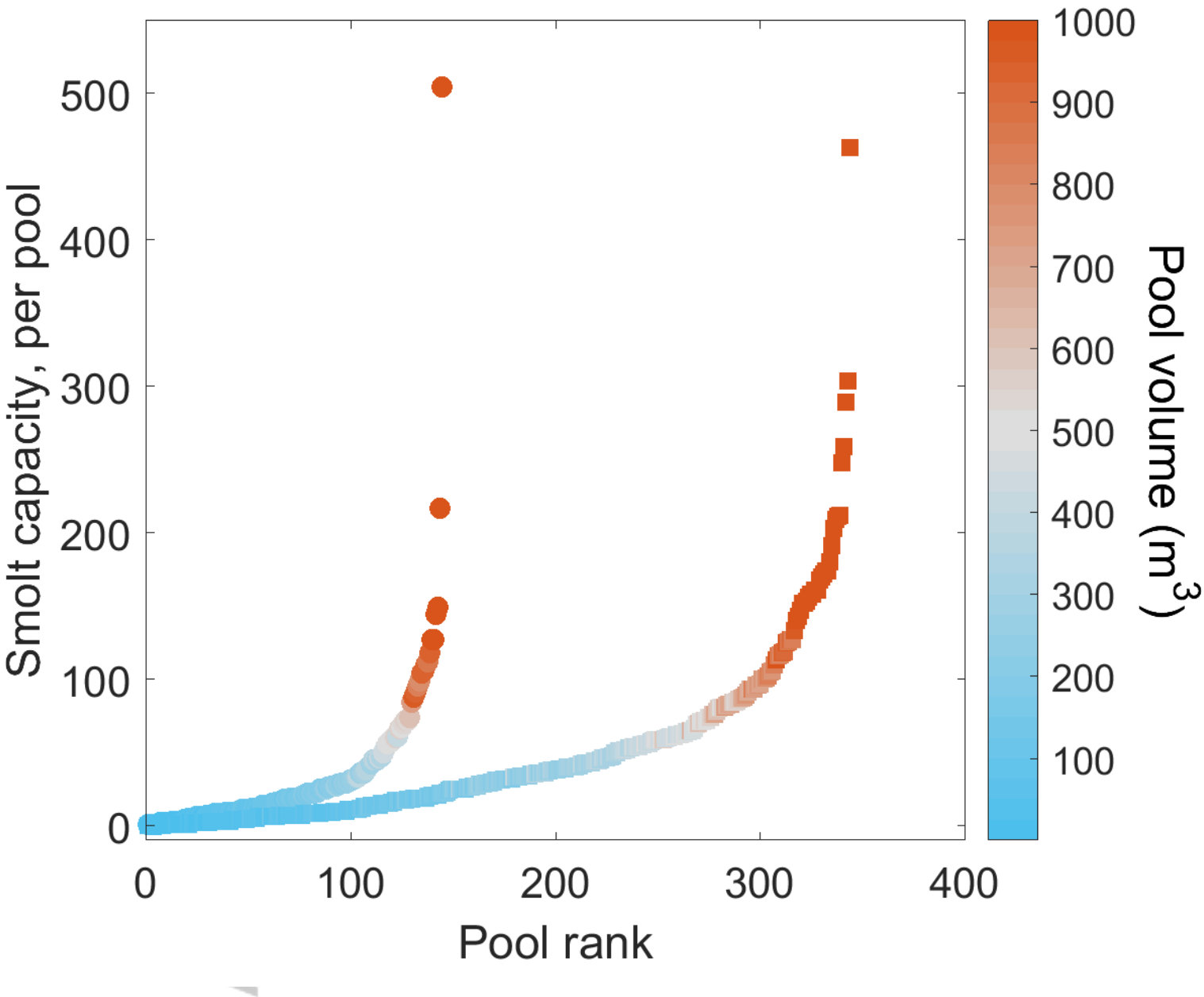

ECO_1845_F6.tif

Table 1. Physical characteristics of the lower Santa Ynez River, CA.

Mean bed gradient	0.0027
Bankfull discharge ($m^3 s^{-1}$)	34
Mean channel width (m)	31.4
Mean floodplain width (m)	242
Mean bankfull depth (m)	1.1
Sinuosity	1.27
Median sediment diameter, D_{50} (m)	0.045

Table 2. Results from depth retrieval calibration and validation.

Year	2010	2011
Calibration R^2	0.74	0.75
Calibration σ_r [a]	0.14	0.15
Validation R^2	0.73	0.70
Validation σ_r	0.15	0.16
Validation intercept	0.022	0.028
Validation slope	0.97	0.98

[a] σ_r, regression standard error